



3-6-6

THE PREDICTION OF HIGH FREQUENCY STRONG GROUND MOTION SPECTRA

Katsuhiko ISHIDA

Central Research Inst. of Electric Power Ind.,
Abiko, Abiko-City, Chiba, Japan

SUMMARY

In this paper, the practical semi-empirical equations based on modified ω^{-2} model for estimating the strong motion spectrum is proposed. The equations are formulated by simple parameters (magnitude (M), hypocentral distance (R) and stress drop ($\Delta\sigma$)). Spectra estimated by the practical equations are compared with observed spectra obtained on rock ($V_S=0.6\sim 1.6$ Km/s) and basement rock ($V_S \simeq 2.5$ Km/s). Accordingly, the estimated acceleration Fourier spectra agree well with the observed ones.

INTRODUCTION

For many engineering design of structures, it is necessary to make a practical model for predicting the high frequency ground motion spectrum. In order to formulate the practical model for predicting the strong motion spectrum, the simple parameters, magnitude(M), hypocentral distance(R), stress drop($\Delta\sigma$), etc., should be considered for engineering aspects. In this paper, the simple semi-empirical equation to predict the acceleration Fourier spectrum is proposed, and is compared with observed spectrum.

SIMPLE SEMI-EMPIRICAL ATTENUATION EQUATION

The synthetic far-field ground motion spectrum of acceleration $F_A(\omega)$ of S wave is obtained from the smoothed rupture velocity model (Ref. 9) as in the following equation;

$$F_A(\omega) = 2 [R_s(\theta, \phi, r) \cdot M_0 \cdot F_2(\omega, \tau_0, \tau_M) \cdot |G| \cdot \omega] \exp\left[-\frac{\omega R}{2Q_S V_S}\right] \cdot \omega^2 \quad (1)$$

where R_s refers to the radiation pattern of the S wave; θ , ϕ , and R are spherical coordinates of the receiver; M_0 is seismic moment; F_2 describes the effects of the finite dimension of the source (bilateral); the factor 2 represents the amplifying effect of the outcrop of a basement rock; the term $\exp\left(-\frac{\omega R}{2Q_S V_S}\right)$ refers to the attenuation of S wave through the wave path; $\tau_0 = (L_0/V_S) [(V_S/V_r)^{-\cos\theta}]$ and $\tau_M = (L_M/V_S) [(V_S/V_r) + \cos\theta]$ (Ref. 9); V_r is rupture velocity; and L_0 and L_M are fault length, respectively. $|G|$ is a Fourier transform of source time function $G(t) = [1 - \exp(-t/T_0)]$. T_0 is a rise time and ω is an angular frequency. R is a distance from a fault plane to a station, V_S is S wave velocity.

In high frequency range, the equation (1) is a flat. In this high frequency range, we can replace $|G|\omega^2$ with $1/T_0$. We can also replace $R_s(\theta, \phi, R)$ with $1/(4\mu V_s^3 \rho R)$ (where $\theta=0^\circ$, $\phi=90^\circ$).

If the rupture propagete unilateraly, we can replace the F_2 with $4V_R/\omega L_0$ (where $V_R=0.72V_s$, $\theta=0^\circ$).

So, we can get following equation by substituting above simplified relations into eq. (1).

$$F_A(T) \approx \frac{1}{4\mu V_s^3 \rho R} \cdot M_0 \cdot \frac{1}{T_0} \quad (4.0) \cdot \frac{V_R}{L_0} \quad (\text{Unilateral}) \quad (2)$$

where $F_A(T)$ is an acceleration Fourier spectrum. T is a period.

We have a following relationships between seismic moment M_0 and magnitude M . We also have relationship between fault length L_0 and magnitude M .

$$\log M_0 = 1.5M + 1.6 \quad (\text{Ref. 5}) \quad (3)$$

$$\log L_0 = 0.5M - 1.8 \quad (\text{Ref. 7}) \quad (4)$$

Considering the corner period T_2^C , the rise time T can be expressed as follows.

$$T = T_2^C / 2\pi \quad (5)$$

We consider the rise time T_0 according to Savage (1972). Accordingly, we can get the following relationship between corner period T_2^C and magnitude M .

$$T_2^C = 10^{0.5M - 2.4} \quad (6)$$

Substituting eqs. (3), (4), (5) and (6) into eq. (2). We can get the following simple semi-empirical acceleration Fourier spectrum at an outcropped basement rock in the period range $T \leq T_2^C$ under the assumption that the S wave velocity is about 3.0 km/s and density ρ is 2.5 g/cm³.

$$\tilde{F}_A(T) \approx 18 \times 10^{0.5M - 2} / R \quad (\text{Unilateral}) \quad (7)$$

If the rupture propagete bilateraly from the center to each end of fault plane, we can go the following equation, replacing $F_2(\omega, \tau_0, \tau_\mu)$ with $2.56 V_R/L_0$.

$$\tilde{F}_A(T) \approx 11.5 \times 10^{0.5M - 2} / R \quad (\text{Bilateral}) \quad (8)$$

Accordingly, we can get a simple equations instead of equation (1) as follows.

$$\tilde{F}_A(T) \approx [18 \times 10^{0.5M - 2} / R] \exp \left\{ - \frac{\omega R}{2V_s Q_s} \right\} \quad (\text{Unilateral}) \quad (9)$$

$$\tilde{F}_A(T) \approx [11.5 \times 10^{0.5M - 2} / R] \exp \left\{ - \frac{\omega R}{2V_s Q_s} \right\} \quad (\text{Bilateral}) \quad (10)$$

It is well known that it is difficult to explain the features of high frequency spectrum by eqs. (1), (9) and (10). In order to explain features of high frequency spectrum, a semi-empirical methodology was proposed under the assumption that the synthetic acceleration Fourier spectrum is nearly equal to that of a low-pass filtered strong ground motion observed at a site as shown in Fig. 1 [Ref. 2, 3]. There, the low-pass filter was determined as follows [Ref. 2, 3]:

$$A(T) = \frac{aT}{aT + 1}, \quad a = 0.023\Delta\sigma + 0.22 \quad (11)$$

where $\Delta\sigma$ is a stress drop.

By using the low-pass filter $A(T)$, the observed acceleration Fourier

spectrum was estimated as following equation.

$$\tilde{B}(T) = \tilde{F}_A(T) / A(T) \quad (12)$$

Substituting eqs. (9) or (10) into eq. (12), the high frequency acceleration Fourier spectrum can be estimated by eqs. (12) and (13).

$$\tilde{B}(T) \simeq \{ [18 \times 10^{0.5M-2} / R] / A(T) \} \exp \left\{ - \frac{\omega R}{2V_s Q_s} \right\} \quad (\text{Unilateral}) \quad (13)$$

$$\tilde{B}(T) \simeq \{ [11.5 \times 10^{0.5M-2} / R] / A(T) \} \exp \left\{ - \frac{\omega R}{2V_s Q_s} \right\} \quad (\text{Bilateral}) \quad (14)$$

$\tilde{B}(T)$ is the observed acceleration Fourier spectrum in short period range on a basement rock.

Generally speaking, it is also necessary to consider the effect of surface geology to estimate the design earthquake input to the structures. In this case, it is necessary to know the amplification factor of the soil, $H(T)$, which should be multiply by eqs. (13) and (14), respectively.

COMPARISONS OF PREDICTED AND OBSERVED ACCELERATION FOURIER SPECTRUM

Accelerograms Obtained at the Basement Rock Figs. 2 and 3 show the comparisons of observed acceleration Fourier spectrum obtained at the basement rock ($V_s \simeq 2.5$ km/s) and estimated ones of Izu-Ohshima kinkai earthquake ($M=7.0$) (1978) and Izu-Hanto Toho-oki earthquake event ($M=6.7$) (1980). The rupture of Izu-Ohshima kinkai earthquake propagated unilaterally, and the rupture of Izu-Hanto Toho-oki earthquake propagated bilaterally. So, eq. (13) should be used for Izu-Ohshima kinkai earthquake, and eq. (14) should be used for Izu-Hanto Toho-oki earthquake event. The stress drops were $\Delta\sigma=66$ bars for Izu-Ohshima kinkai earthquake and $\Delta\sigma=48$ bars for Izu-Hanto kinkai earthquake, respectively.

Observatories in the deep wells (Ref. 6) were installed in basement rock ($V_s \simeq 2.5$ km/s), so the strong motion acceleration Fourier spectra estimated by eqs. (14) or (15) should be reduced to half.

Accelerograms Obtained at Outcropped Rock Fig. 4 shows the result of analysis of Nihonkai-Chubu earthquake of 1983 and after shock of it.

This event was the typical multiple shock. The main shock had two fault planes (Ref. 8). The two parts (b, c) indicated in the Fig. 4 correspond to each fault plane. The stress drop of each part (b, c) were estimated to be $\Delta\sigma=70$ bars (for b part) and $\Delta\sigma=36$ bars (for c part) (Ref. 8).

Fig. 5 shows the results of two aftershocks ($M=7.1$ and $M=6.1$) of the Nihonkai-Chubu earthquake. The stress drop of each event are indicated in the figure. If the amplification factor of the surface layer $H(T)$ assumed to be 2, observed acceleration Fourier spectrum of main shock and aftershock agree well with the predicted ones.

Fig. 6 shows the comparison of observed acceleration Fourier spectrum and predicted one of Kanto earthquake ($M=7.1$) of 1923. Fig. 7 shows the result of Saitama earthquake ($M=6.1$) of 1968. The rupture of these two events (Kanto earthquake and Saitama earthquake) propagated unilaterally.

The observed acceleration Fourier spectrum agree well with the estimated results.

CONCLUSION

In order to approve the applicability of proposed semi-empirical formulas, the accelerograms of earthquake events obtained at rock were analyzed. Accordingly, it will be possible to estimate approximately the characteristics of the acceleration Fourier spectrum considering the faulting by using eq. (13) or eq. (14).

REFERENCE

1. Abe, K., Static and Dynamic Fault Parameters of the Earthquake of July, 1, 1968, Tectonophysics, vol. 27, 223-238, (1975)
2. Ishida, K., Approximate method to Estimate the Short-period Strong Motion Spectra on Bedrock, Bulletin of the Seism. Soc. Amer., vol. 71, 491-505, (1981)
3. Ishida, K., A Study on the Estimate the Characteristics of the Strong Motion Spectra, Trans. Arch. Inst. Japan, vol. 314, 48-58, (1982)
4. Kanamori, H., Faulting of the Great Kanto Earthquake of 1923 Revealed by Seismological Data, Bull. Earth. Res. Inst., vol. 49, 13-18, (1971a)
5. Kasahara, K., Standard Values of Fault Parameters, Abstract, The Seism. Soc. Japan, (1975)
6. Kinoshita, S., Spectral Characteristics of Bedrock Motions in Tokyo Metropolitan Area, JSCE, 344, 89-94, (1984)
7. Otsuka, M., Earthquake Magnitude and Fault Formation, J. Phys. Earth., 12, (1964)
8. Sato, T., Rupture Characteristics of the 1983 Nihonkai-Chubu Earthquake as Inferred from Strong Motion Accelerograms, J.P.E. 33, 525-557, (1985)
9. Savage, J.C., Relation of Corner Frequency to Fault Dimensions, Res. vol. 77, 3788-3795, (1972)
10. Shimazaki, K. and P. Somerville (1978), Summary of the Static and Dynamic Parameters of the Izu-Ohshima Kinkai Earthquake of January 14, 1978, Bull. Earth. Res. Inst. vol. 53, 613-628.

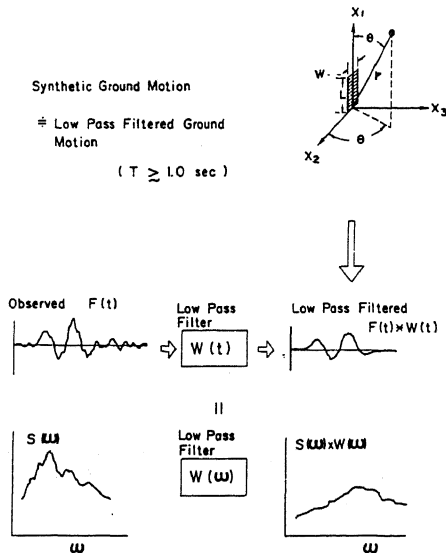


Fig. 1a Schematic explanation of basic assumption. The synthetic ground motion calculated from Haskell model is assumed to be nearly equal to a low-pass filtered ground motion.

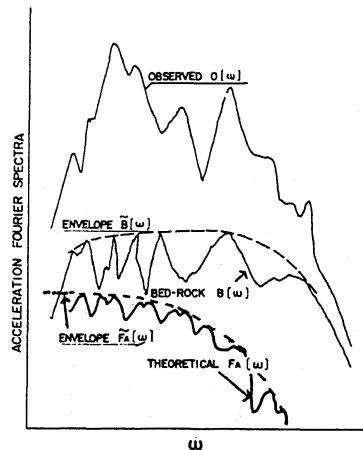


Fig. 1b The overall relation between $O(\omega)$, $B(\omega)$ and $F_A(\omega)$. $\tilde{F}_A(\omega)$ and $\tilde{B}(\omega)$ show the envelope spectra of $F_A(\omega)$ and $B(\omega)$, respectively.

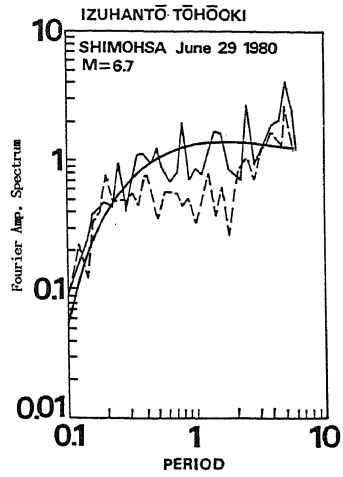
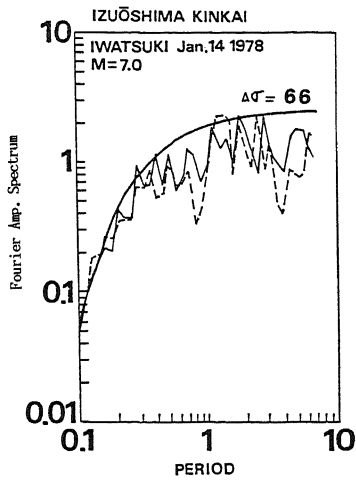


Fig.2 Comparison of the estimated acceleration Fourier spectrum and observed ones of Izu-Oshima Kinkai earthquake(1978).

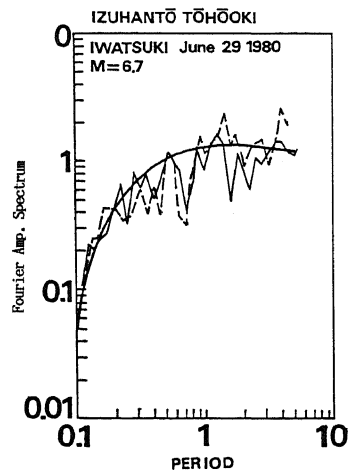
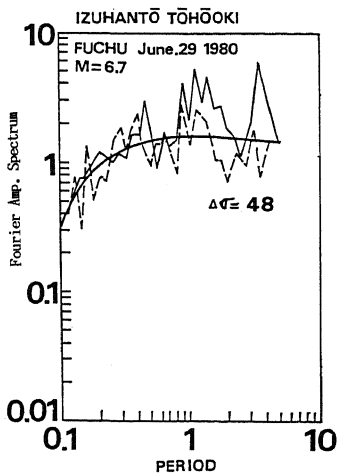


Fig.3 Comparisons of the estimated acceleration Fourier spectrum and observed one of Izu-Hanto Toho-Oki earthquake(1980). Observed spectrum in each figure indicate the two horizontal components.

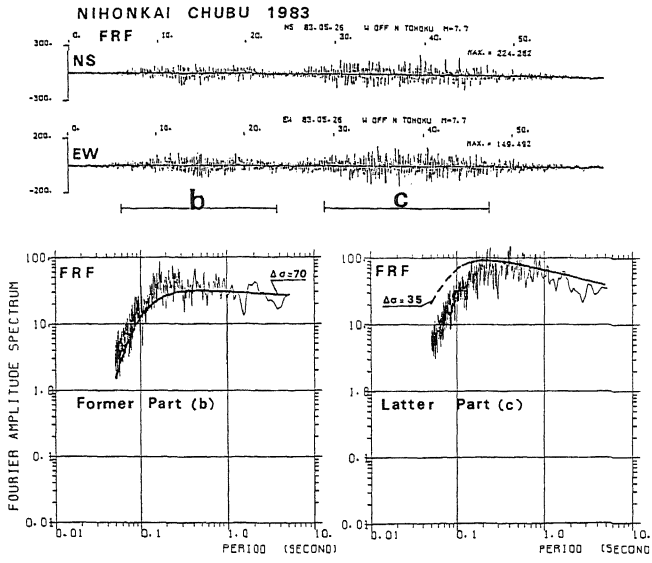


Fig.4 Comparisons of the estimated acceleration Fourier spectrum and observed ones of Nihonkai-Chubu earthquake(1983)(main shock).

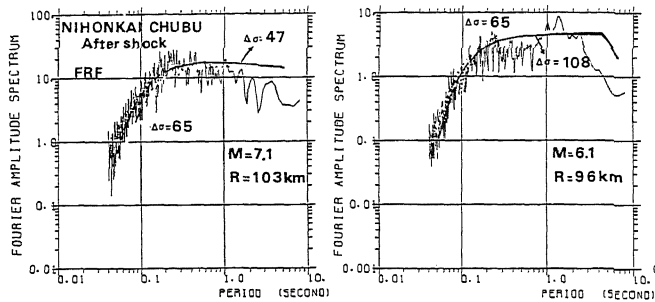


Fig.5 Comparisons of the estimated acceleration Fourier spectrum and observed ones of after shock of 1983 Nihonkai-Chubu earthquake.

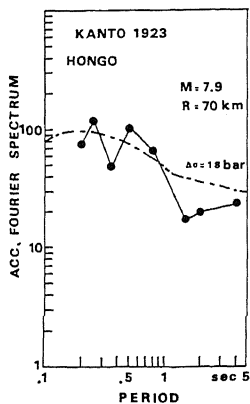


Fig.6 Comparison of the estimated acceleration Fourier spectra and observed ones of 1923 Kanto earthquake.

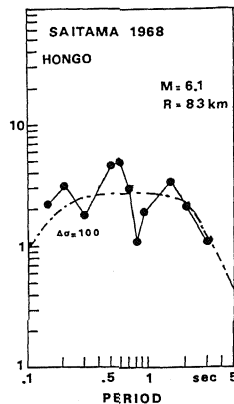


Fig.7 Comparison of the estimated acceleration Fourier spectra and observed one of 1968 Saitama earthquake.